Published in final edited form as:
Am J Ophthalmol. 2010 December ; 150(6): 849–855. doi:10.1016/j.ajo.2010.06.034.

Thickness Mapping of Retinal Layers by Spectral Domain Optical Coherence Tomography

Ana L. LoDuca, **Chi Zhang**, **Ruth Zelkha**, and **Mahnaz Shahidi**
Department of Ophthalmology & Visual Sciences, University of Illinois at Chicago

Introduction

Optical coherence tomography (OCT) is an optical imaging technique that provides objective and quantitative measurements of retinal thickness alterations associated with retinal diseases. OCT images have been analyzed to provide maps of normal macular thickness.[1] Furthermore, segmentation of OCT images has provided information about thickness of specific retinal layers. Time domain (TD) OCT images have been segmented to provide thickness maps of the nerve fiber layer, ganglion cell layer, inner plexiform layer, and inner nuclear layer in normal subjects and glaucoma patients.[2, 3] Additionally, thickness maps of the outer nuclear layer have been generated in normal subjects and in children with Leber's congenital amaurosis.[4] Furthermore, ultra-high resolution OCT imaging has been applied to measure thickness of the photoreceptor layer in normal subjects and patients with macular degeneration.[5, 6]

With the availability of spectral domain OCT (SD OCT), it is now possible to obtain multiple scans over a retinal area and generate quantitative maps of retinal thickness with high spatial resolution. Several studies have reported comparisons of total retinal thickness measurements obtained by TD and SD OCT instruments.[7–9] Additionally, SD OCT imaging technology has been used to measure macular thickness in normal subjects[8, 10, 11] and to generate macular thickness maps of a three-layer complex consisting of the nerve fiber layer, ganglion cell layer and inner plexiform layer in patients with various non-glaucomatous optic neuropathies.[12] In the current study, our previously reported SD OCT image segmentation technique[13] was applied to SD OCT images. Normal thickness maps of 6 retinal layers were generated and intersubject thickness variations were assessed. For each retinal layer, thickness measurements and variations in 9 macular sectors were established. Generating normal thickness maps of retinal layers and assessing thickness variations among subjects is needed to identify thickness changes that occur due to disease.

Corresponding Author Mahnaz Shahidi, Ph.D., Department of Ophthalmology and Visual Sciences, University of Illinois at Chicago, 1855 West Taylor Street, Chicago IL 60612, Tel: 312-413-7364, Fax: 312-413-7366, mahnshah@uic.edu.

[b]Financial Disclosures (including none): None

[c]*Contributions to Authors in each of these areas:* Design of the study (MS); Conduct of the study (MS); collection, management, analysis, and interpretation of the data (AL, CZ, RZ, MS); preparation, review, or approval of the manuscript (AL, MS).

[d]*Statement about Conformity with Author Information:* The study was approved by the University of Illinois at Chicago IRB and proper informed consent for participation in the research and HIPAA compliance were obtained.

Materials and Methods

Approval for use of human subjects in the research study was obtained from an institutional review board of the University of Illinois at Chicago. The study was explained to the subjects, and informed consents were obtained according to the tenets of the Declaration of Helsinki. SD OCT imaging was performed in one eye of 15 normal subjects, 8 female and 7 male, 8 right and 7 left eyes. The subjects' ages ranged between 40 and 59 years, with an average age of 52 ± 6 years (mean ± standard deviation).

SD OCT imaging was performed using a commercially available OCT instrument (Spectralis, Heidelberg Engineering, Germany). Nineteen horizontal SD OCT B scans were acquired in each eye, encompassing a 6 mm X 5 mm retinal area, centered on the fovea. Each SD OCT image was 1024 pixels (6 mm) in length and 496 pixels (2 mm) in depth. The grayscale SD OCT images were exported in tagged image file format for segmentation analysis.

Each SD OCT image was analyzed using an image segmentation algorithm and thickness profiles of 6 retinal layers were automatically generated, as previously described.[13] A representative SD OCT image obtained in one subject is shown in Fig 1. Six retinal layers were identified by the automatic segmentation algorithm: nerve fiber layer (layer 1), ganglion cell layer + inner plexiform layer (layer 2), inner nuclear layer (layer 3), outer plexiform layer (layer 4), outer nuclear layer + photoreceptor inner segments (layer 5), and photoreceptor outer segments (layer 6). The image segmentation algorithm was applied to all 19 SD OCT images. From each image, a thickness profile for each of the 6 retinal layers was generated by averaging thickness over contiguous 240-micron segments, along the 6 mm scan length. Layer 1 thickness profiles derived from all images were combined to generate a thickness map of layer 1. This procedure was repeated for each of the 6 retinal layers. Thickness maps of the 6 retinal layers were displayed in pseudo color. Total retinal thickness was also calculated by summing thickness measurements in the 6 layers.

From the retinal layer thickness map, data were grouped in 9 macular sectors within 3 concentric circles as defined by the Early Treatment Diabetic Retinopathy Study.[14] The retinal areas encompassed by the 9 macular sectors are displayed in Fig 2. In each subject, the location of the center of fovea was first identified based on the minimum thickness on the map of layer 2 (ganglion cell layer + inner plexiform layer). This location defined the center of the concentric circles. Since the thickness data was stored in a 2 dimensional rectangular array, the horizontal dimension was used to define the diameter of the circles for grouping of data points. The central circle (sector 1) had a diameter of 1.2 mm and represented the central foveal area. The second circle had a diameter of 3.1 mm and was sub-divided into superior (sector 2), nasal (sector 3), inferior (sector 4) and temporal (sector 5) parafoveal retinal areas. The third circle had a diameter of 6 mm and was subdivided into superior (sector 6), nasal (sector 7), inferior (sector 8) and temporal (sector 9) perifoveal retinal areas. Macular sectors 1, 2 to 5, and 6 to 9 contained 15, 38 and 74 data points, respectively.

From thickness maps generated in each subject, a mean and standard deviation (SD) of measurements was calculated in each of the 9 macular sectors and 6 retinal layers. Intrasector variability was defined by a mean SD of thickness measurements, averaged over all subjects. From thickness maps generated in all subjects, a mean normal thickness was established in each of the 9 macular sectors and in each of the 6 layers, by averaging thickness measurements over all subjects. Intersubject variability was defined as the SD of thickness measurements in all subjects. Thickness measurements among sectors were compared in each layer using analysis of variance statistics. Total retinal thickness in each

sector was calculated by summing thickness measurements in all 6 layers. In the same subjects, an average total retinal thickness in each macular sector was obtained from the Spectralis SD OCT software. Total retinal thickness measurements, averaged over all macular sectors, obtained by automated mapping and Spectralis SD OCT software were compared, using linear regression analysis.

Results

By automated segmentation of 19 SD OCT images, thickness maps were generated in 6 retinal layers: nerve fiber layer (layer 1), ganglion cell layer + inner plexiform layer (layer 2), inner nuclear layer (layer 3), outer plexiform layer (layer 4), outer nuclear layer + photoreceptor inner segments (layer 5), and photoreceptor outer segments (layer 6). Examples of thickness maps generated from the right eye of one subject are shown in Fig 3. The thickness map of layer 1 (nerve fiber layer) displayed minimum thickness in the central foveal area and maximum thickness nasal to the fovea. The thickness map of layer 2 (ganglion cell layer + inner plexiform layer) also displayed a minimum thickness in the central foveal area, but the maximum thickness was observed in a circular pattern in the parafoveal retinal area. The thickness map of layer 3 (inner nuclear layer) showed a relatively constant thickness, with the lowest thickness in the central foveal area. In the foveal and parafoveal retinal areas, thickness of the layer 4 (outer plexiform layer) was highest and relatively constant, while in the perifoveal retinal area, thickness was lower and also relatively constant. Thickness of layer 5 (outer nuclear layer + photoreceptor inner segments) was highest in the central foveal area and relatively constant in the parafoveal and perifoveal retinal areas. The thickness map of layer 6 (photoreceptor outer segments) displayed a uniform thickness in all retinal areas.

Mean macular sector thickness for each of the 6 retinal layers and the corresponding SD (intersubject thickness variability) is shown in Fig 4 (displayed for a right eye). Nerve fiber layer thickness superior and inferior to the fovea was similar. A minimum thickness of the nerve fiber layer was observed in the central foveal area and a maximum thickness in the perifoveal retinal area, nasal to the fovea and closest to the optic nerve head. Thickness of the ganglion cell layer + inner plexiform layer was highest in parafoveal retinal areas, particularly nasal to the fovea. The inner nuclear layer thickness was relatively constant in all macular sectors, with a minimum thickness observed in the central foveal area. The outer plexiform layer thickness was also relatively constant in foveal and parafoveal retinal areas and higher than the uniform thickness measured in perifoveal retinal areas. The outer nuclear layer + photoreceptor inner segments thickness map displayed a maximum thickness in the central foveal area and a relatively constant thickness in the perifoveal retinal areas. Thickness of the photoreceptor outer segments layer was slightly higher in the central foveal area, but overall relatively constant in all macular sectors.

Intersubject thickness variability, defined as the SD of thickness measurements in each macular sector and each retinal layer is displayed in Fig 4. The mean and SD of thickness measurements in each retinal layer are plotted as a function of eccentricity in Fig 5. In the nerve fiber layer, the largest thickness variation among subjects was observed in the perifoveal nasal retinal area, which also had the highest mean thickness. Intersubject thickness variability of the ganglion cell layer + inner plexiform layer was largest in parafoveal retinal areas, indicating large individual variations in this region. In the inner nuclear and outer plexiform layers, thickness variations among subjects were relatively uniform across all macular sectors and also lowest compared to all other layers. Intersubject thickness variability in the outer nuclear layer + photoreceptor inner segments layer was largest superior and inferior to the fovea and relatively constant in other macular sectors.

Thickness variations among subjects in all macular sectors of the photoreceptor outer segments layer were relatively constant.

Intrasector thickness variability, defined by the mean SD of thickness measurements (averaged over all subjects) in each macular sector and retinal layer is listed in Table 1. In the nerve fiber layer, the largest intrasector variability was observed in the perifoveal retinal area superior, nasal and inferior to the fovea. Intrasector thickness variability of the ganglion cell layer + inner plexiform layer was largest compared to all other layers. In the inner nuclear layer, intrasector thickness variation was greatest in central foveal area and relatively constant in all other sectors. Intrasector thickness variabilities in the outer plexiform layer and outer nuclear layer + photoreceptor inner segments layer were similar, with the largest variations observed in the central foveal area and perifoveal retinal area nasal to the fovea. In the photoreceptor outer segments layer, intrasector thickness variability was small and relatively constant in all macular sectors. Thickness measurements among 9 macular sectors were significantly different in all layers ($p < 0.001$), except the photoreceptor outer segments layer ($p = 0.5$).

The relationship between total retinal thickness derived from thickness mapping and Spectralis SD OCT software is shown in Fig 6. There was a significant correlation between total thickness measured by thickness mapping and Spectralis SD OCT software ($r = 0.90$, $p < 0.001$; $N = 15$). The best fit line relating total retinal thickness derived by the two methods had the following equation: Thickness (segmentation) = 0.94 * Thickness (Spectralis software).

Discussion

Thickness mapping of retinal layers can be useful for detection and monitoring of thickness alteration in specific retinal layers associated with retinal pathologies. In the current study, application of a novel automated image segmentation technique for thickness mapping of 6 retinal layers using SD OCT technology was reported. Thickness maps generated in normal subjects corresponded with normal retinal anatomy. Total retinal thickness derived by automated thickness mapping highly correlated with measurements obtained by Spectralis SD OCT commercial software. In addition, normal retinal thickness maps for 6 retinal layers were generated, intersubject thickness variability was established, and normal thickness variations in 9 macular sectors of each layer were reported.

Thickness maps of the nerve fiber layer and ganglion cell layer + inner plexiform layer displayed a minimum in the central foveal area, as expected with normal anatomy. The nerve fiber layer thickness was highest in the perifoveal retinal area (near the optic nerve head), due to the high density of nerve fiber bundles near the optic nerve head. Intersubject variability was 11 microns (19%), indicative of large individual variations in normal nerve fiber layer thickness. The ganglion cell layer + inner plexiform layer thickness was greatest in the parafoveal retinal area, particularly nasal to the fovea, due to the papillomacular bundle. Intersubject variability was largest in the parafoveal retinal area and on average 11 microns (12%). Intrasector thickness variability of ganglion cell layer + inner plexiform layer was largest compared to all other layers. The inner nuclear layer displayed a minimum thickness in the central foveal and intersubject variability was on average 3 microns (8%). Thickness of the outer plexiform layer was relatively uniform and intersubject variability was on average 5 microns (15%). In the central foveal area, thickness maps of the outer nuclear layer + photoreceptor inner segments displayed a maximum, which is expected anatomically, partially due to the elongated foveal cone photoreceptors. Intersubject variability was on average 9 microns (11%). Thickness variability in the photoreceptor outer segments layer was on average 7 microns (18%), indicative of large variations in

photoreceptor cell structure among normal subjects. Intrasector thickness variability of the photoreceptor outer segments layer was on average 5 microns, suggesting uniform thickness across all retinal areas.

Mean nerve fiber layer thickness averaged over all macular sectors was 36 ± 7 microns, comparable to 30 ± 5 microns previously reported by TD OCT imaging.[15] Mean nerve fiber layer thickness averaged over all macular sectors, excluding the central foveal area, was 40 ± 7 microns, in agreement with measurements of 34 ± 5 microns obtained by SD OCT,[3] but higher compared to previously reported measurements (28 ± 5 microns)[2] obtained by low resolution TD OCT. Mean thickness of the ganglion cell layer + inner plexiform layer and inner nuclear layer averaged over all sectors, excluding the central foveal area, were 72 ± 9 and 34 ± 2 microns, respectively, similar to previously published measurements of 73 ± 7 and 33 ± 3 microns, respectively.[3] However, mean ganglion cell layer + inner plexiform layer + inner nuclear layer thickness (106 ± 10 microns) was higher than previously reported thickness measurements of the inner retina complex (91 ± 4 microns).[2] Compared to previous studies that analyzed 6 radial TD OCT images, inner retina thickness measurements in the current study were similar to one study[3] and consistently higher than a second study.[2] The disparity in thickness measurements may be attributed to differences in image resolution and segmentation algorithms. Thickness maps of the nerve fiber layer + ganglion cell layer + inner nuclear layer in the current study displayed similar thickness variations as compared to those generated by a prototype SD OCT instrument.[12]

The pattern of thickness variations on outer nuclear layer maps in the current study corresponded well with those generated in a previous study.[4] Mean outer nuclear layer + photoreceptor inner segments + photoreceptor outer segments thickness (115 ± 8 microns) was higher than previously reported thickness measurements of outer retina complex (ORC) (96 ± 6 microns), using ultra-high resolution OCT and thickness mapping based on 6 radial scans.[5] Since the ratio of ORC to total retinal thickness was similar in both studies, the difference in ORC thickness may be attributed to variations in segmentation algorithms in detecting the posterior retinal boundary. A recent study has established an increased measurement of total retinal thickness by Spectralis SD OCT as compared to Stratus TD OCT, due a difference in detection of the photoreceptor outer segment / retinal pigment epithelium (RPE) interface.[9]

Total retinal thickness derived by thickness mapping was highly correlated with measurements obtained by Spectralis SD OCT software, but consistently lower (~6%). This difference may be attributed to the dissimilarity in the location of the posterior retinal boundary detected using the two methods. Spectralis SD OCT software included the outer segment / RPE-Bruch's membrane complex in thickness measurements,[9] while the automated segmentation algorithm in the current study detected the inner border of the complex as the posterior retinal boundary. In the foveal area, total retinal thickness in the current study (264 ± 13) was comparable to previously reported data in normal subjects (270 ± 23).[10] A comparison of total retinal thickness in each of 9 macular sectors obtained by various SD OCT instruments[8, 11] and the current study is shown in Table 2. Despite the differences in populations, thickness measurements are similar.

In summary, a method for automated thickness mapping of 6 retinal layers is reported. Normal thickness maps for each layer were generated and thickness variabilities among subjects and macular areas were assessed. SD OCT image segmentation and retinal thickness mapping may be limited in the presence of retinal pathologies that cause local changes in the optical properties of retinal layers and requires further investigation. Overall, the application of this technique is promising for investigating thickness changes in specific retinal layers and macular areas attributable to disease.

Acknowledgments

a. *Funding / Support (including none):* Department of Veterans Affairs, Washington, DC, NIH grants EY14275 and EY01792, Bethesda, Maryland; senior scientific investigator award and an unrestricted departmental grant from Research to Prevent Blindness, Inc., New York, New York.

e. Other Acknowledgments: None.

References

1. Chan A, Duker JS, Ko TH, Fujimoto JG, Schuman JS. Normal macular thickness measurements in healthy eyes using Stratus optical coherence tomography. Arch Ophthalmol 2006;124(2):193–8. [PubMed: 16476888]
2. Ishikawa H, Stein DM, Wollstein G, Beaton S, Fujimoto JG, Schuman JS. Macular segmentation with optical coherence tomography. Invest Ophthalmol Vis Sci 2005;46(6):2012–7. [PubMed: 15914617]
3. Tan O, Li G, Lu AT, Varma R, Huang D. Mapping of macular substructures with optical coherence tomography for glaucoma diagnosis. Ophthalmology 2008;115(6):949–56. [PubMed: 17981334]
4. Jacobson SG, Cideciyan AV, Aleman TS, et al. Photoreceptor layer topography in children with leber congenital amaurosis caused by RPE65 mutations. Invest Ophthalmol Vis Sci 2008;49:4573–7. [PubMed: 18539930]
5. Chan A, Duker JS, Ishikawa H, Ko TH, Schuman JS, Fujimoto JG. Quantification of photoreceptor layer thickness in normal eyes using optical coherence tomography. Retina 2006;26(6):655–60. [PubMed: 16829808]
6. Witkin AJ, Ko TH, Fujimoto JG, et al. Ultra-high resolution optical coherence tomography assessment of photoreceptors in retinitis pigmentosa and related diseases. Am J Ophthalmol 2006;142(6):945–52. [PubMed: 17157580]
7. Knight OJ, Chang RT, Feuer WJ, Budenz DL. Comparison of retinal nerve fiber layer measurements using time domain and spectral domain optical coherent tomography. Ophthalmology 2009;116(7):1271–7. [PubMed: 19395086]
8. Sull AC, Vuong LN, Price LL, et al. Comparison of spectral/Fourier domain optical coherence tomography instruments for assessment of normal macular thickness. Retina 2010;30(2):235–45. [PubMed: 19952997]
9. Grover S, Murthy RK, Brar VS, Chalam KV. Comparison of retinal thickness in normal eyes using Stratus and Spectralis Optical Coherence Tomography. Invest Ophthalmol Vis Sci 2010;51(5):2644–7. [PubMed: 20007831]
10. Grover S, Murthy RK, Brar VS, Chalam KV. Normative data for macular thickness by high-definition spectral-domain optical coherence tomography (spectralis). Am J Ophthalmol 2009;148(2):266–71. [PubMed: 19427616]
11. Ooto S, Hangai M, Sakamoto A, et al. Three-dimensional profile of macular retinal thickness in normal Japanese eyes. Invest Ophthalmol Vis Sci 2010;51(1):465–73. [PubMed: 19696169]
12. Choi SS, Zawadzki RJ, Keltner JL, Werner JS. Changes in cellular structures revealed by ultra-high resolution retinal imaging in optic neuropathies. Invest Ophthalmol Vis Sci 2008;49(5):2103–19. [PubMed: 18436843]
13. Bagci AM, Shahidi M, Ansari R, Blair M, Blair NP, Zelkha R. Thickness profiles of retinal layers by optical coherence tomography image segmentation. Am J Ophthalmol 2008;146(5):679–87. [PubMed: 18707672]
14. Early Treatment Diabetic Retinopathy Study design and baseline patient characteristics. ETDRS report number 7. Ophthalmology 1991;98(5 Suppl):741–56. [PubMed: 2062510]
15. Leung CK, Chan WM, Yung WH, et al. Comparison of macular and peripapillary measurements for the detection of glaucoma: an optical coherence tomography study. Ophthalmology 2005;112(3):391–400. [PubMed: 15745764]

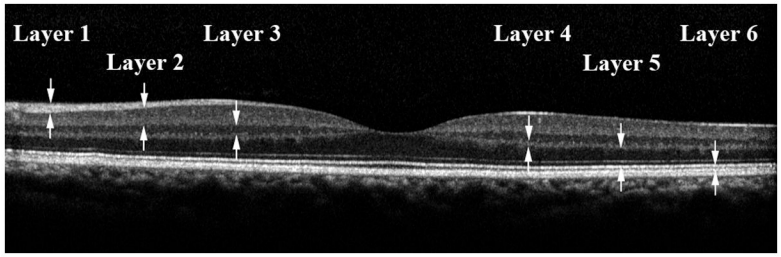

Figure 1.

A representative spectral domain optical coherence tomography image obtained in the left eye of one subject in the study. The 6 retinal were the nerve fiber layer (layer 1), ganglion cell layer + inner plexiform layer (layer 2), inner nuclear layer (layer 3), outer plexiform layer (layer 4), outer nuclear layer + photoreceptor inner segments (layer 5), and photoreceptor outer segments (layer 6).

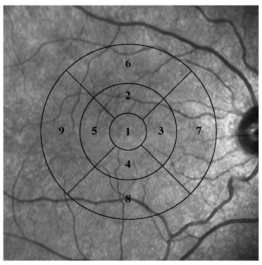

Figure 2.
Thickness data from the map of each layer were grouped in 9 macular sectors, within 3 concentric circles. The retinal areas encompassed by 9 macular sectors are displayed on a fundus photograph.

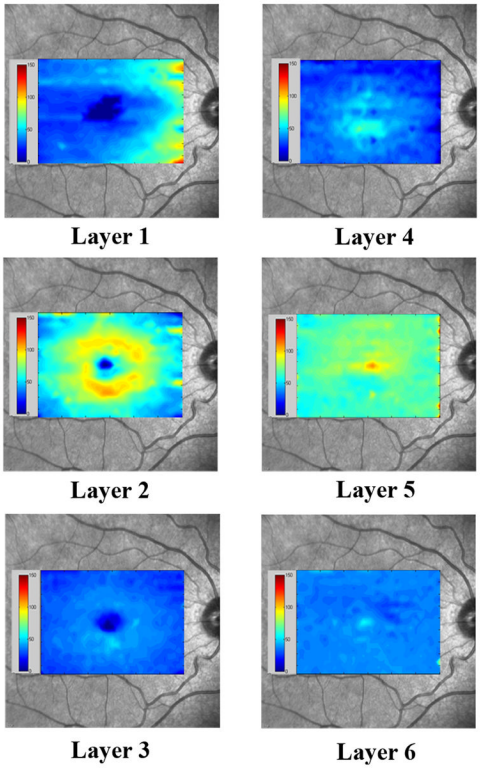

Figure 3.
Examples of thickness maps of 6 retinal layers in a right eye of one subject in the study. The 6 retinal layers were the nerve fiber layer (layer 1), ganglion cell layer + inner plexiform layer (layer 2), inner nuclear layer (layer 3), outer plexiform layer (layer 4), outer nuclear layer + photoreceptor inner segments (layer 5), and photoreceptor outer segments (layer 6).

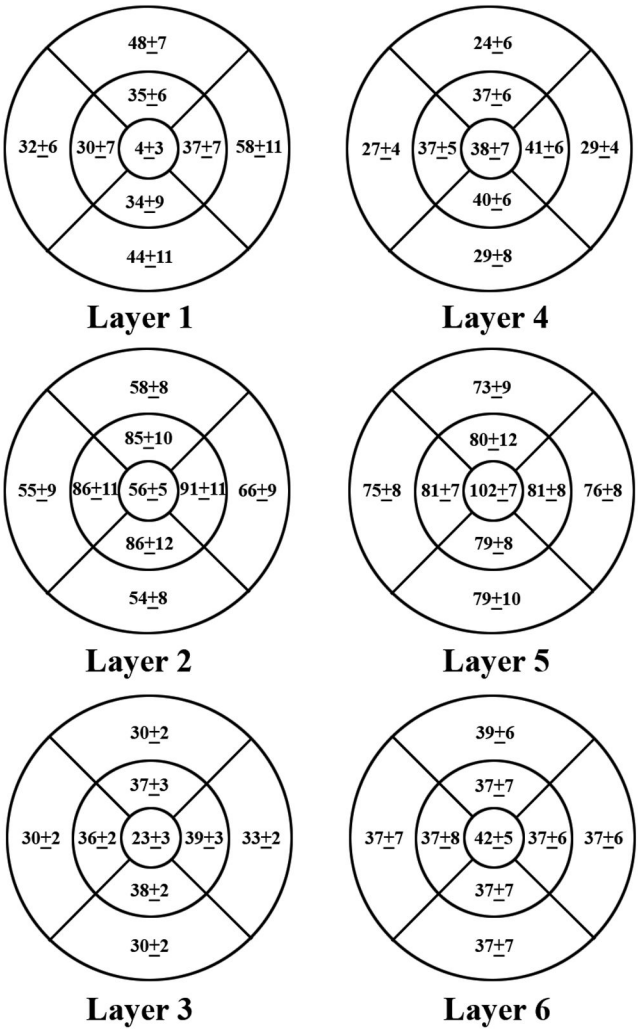

Figure 4.

Mean normal macular sector thickness for 6 retinal layers and the corresponding standard deviations. The 6 retinal layers were the nerve fiber layer (layer 1), ganglion cell layer + inner plexiform layer (layer 2), inner nuclear layer (layer 3), outer plexiform layer (layer 4), outer nuclear layer + photoreceptor inner segments (layer 5), and photoreceptor outer segments (layer 6).

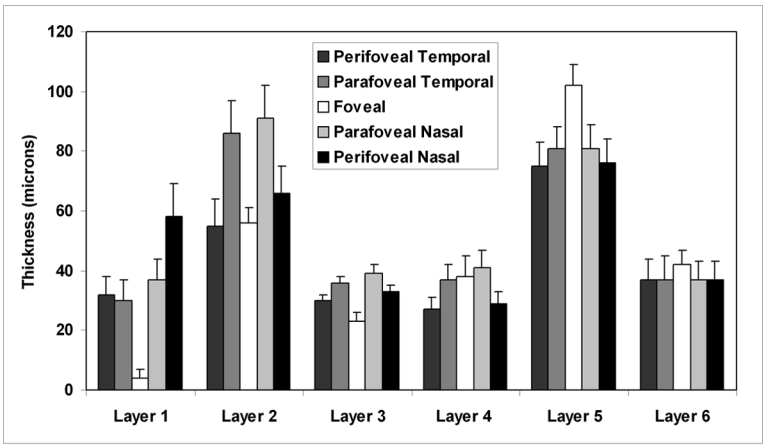

Figure 5.

Mean and standard deviation of macular sector thickness plotted as a function of retinal eccentricity for 6 retinal layers. The 6 retinal layers were the nerve fiber layer (layer 1), ganglion cell layer + inner plexiform layer (layer 2), inner nuclear layer (layer 3), outer plexiform layer (layer 4), outer nuclear layer + photoreceptor inner segments (layer 5), and photoreceptor outer segments (layer 6).

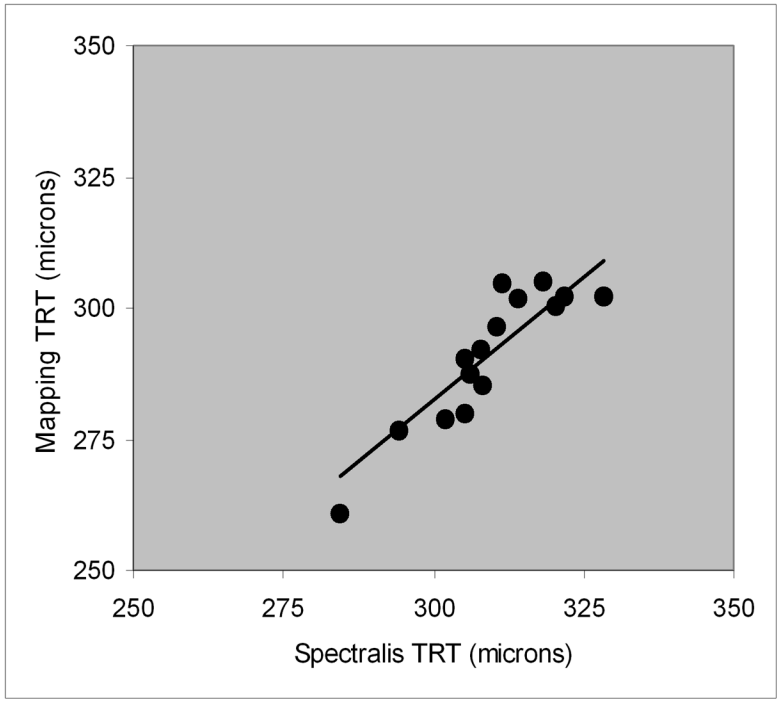

Figure 6.
Relationship between total retinal thickness (TRT) measurements derived by thickness mapping and Spectralis SD OCT software.

Table 1

Intrasector thickness variability in 9 macular sectors: fovea (sector 1); parafoveal superior (sector 2), nasal (sector 3), inferior (sector 4), temporal (sector 5); perifoveal superior (sector 6), nasal (sector 7), inferior (sector 8), temporal (sector 9), and in 6 retinal layers: nerve fiber layer (layer 1), ganglion cell layer + inner plexiform layer (layer 2), inner nuclear layer (layer 3), outer plexiform layer (layer 4), outer nuclear layer + photoreceptor inner segments (layer 5), and photoreceptor outer segments (layer 6).

Mean Standard Deviation (microns)						
	Layer 1	**Layer 2**	**Layer 3**	**Layer 4**	**Layer 5**	**Layer 6**
Sector 1	6	25	9	11	15	5
Sector 2	11	14	4	8	9	5
Sector 3	9	11	4	6	8	5
Sector 4	11	16	4	8	6	4
Sector 5	9	13	2	6	8	4
Sector 6	16	16	6	7	9	6
Sector 7	16	18	6	10	14	7
Sector 8	15	15	6	8	11	6
Sector 9	6	14	4	7	9	7

Table 2

Comparison of total retinal thickness measurements in 9 macular sectors obtained using spectral domain optical coherence tomography instruments. Mean (SD) of thickness measurements are shown in microns.

	Spectralis[1]	Cirrus[2]	RTVue[2]	3D OCT[2]	3D OCT[3]
Macular Sector					
Fovea	264(13)	262(16)	256(15)	231(16)	222(18)
Parafovea					
Temporal	306(14)	306(10)	308(13)	280(10)	285(14)
Superior	311(14)	320(12)	324(11)	293(12)	297(15)
Nasal	325(15)	323(12)	324(11)	296(12)	299(15)
Inferior	314(13)	316(11)	318(10)	288(10)	294(15)
Perifovea					
Temporal	256(14)	255(9)	265(10)	234(16)	244(12)
Superior	271(18)	274(13)	278(13)	249(13)	257(13)
Nasal	298(19)	293(13)	291(14)	266(13)	273(14)
Inferior	274(17)	264(11)	267(12)	240(12)	247(13)

[1] Current Study

[2] Sull et al. [8]

[3] Ooto et al. [11]